Evaluation of therapeutic effects of natural killer (NK) cell-based immunotherapy in mice using *in vivo* apoptosis bioimaging with a caspase-3 sensor

Ho Won Lee,* Thoudam Debraj Singh,* Sang-Woo Lee,* Jeoung-Hee Ha,† Alnawaz Rehemtulla,‡ Byeong-Cheol Ahn,* Young Hyun Jeon,*,[1] and Jaetae Lee*,[1]

*Department of Nuclear Medicine and †Department of Pharmacology, Kyungpook National University, Daegu, Korea; and ‡Department of Radiation Oncology, University of Michigan, Ann Arbor, Michigan, USA

ABSTRACT **Natural killer (NK) cell-based immunotherapy is a promising strategy for cancer treatment, and caspase-3 is an important effector molecule in NK cell-mediated apoptosis in cancers. Here, we evaluated the antitumor effects of NK cell-based immunotherapy by serial noninvasive imaging of apoptosis using a caspase-3 sensor in mice with human glioma xenografts. Human glioma cells expressing both a caspase-3 sensor as a surrogate marker for caspase-3 activation and *Renilla* luciferase (*Rluc*) as a surrogate marker for cell viability were established and referred to as D54-CR cells. Human NK92 cells were used as effector cells. Treatment with NK92 cells resulted in a time- and effector number-dependent increase in bioluminescence imaging (BLI) activity of the caspase-3 sensor in D54-CR cells *in vitro*. Caspase-3 activation by NK92 treatment was blocked by Z-VAD treatment in D54-CR cells. Transfusion of NK92 cells induced an increase of the BLI signal by caspase-3 activation in a dose- and time-dependent manner in D54-CR tumor-bearing mice but not in PBS-treated mice. Accordingly, sequential BLI with the Rluc reporter gene revealed marked retardation of tumor growth in the NK92-treatment group but not in the PBS-treatment group. These data suggest that noninvasive imaging of apoptosis with a caspase-3 sensor can be used as an effective tool for evaluation of therapeutic efficacy as well as for optimization of NK cell-based immunotherapy.—Lee, H. W., Singh, T. D., Lee, S.-W., Ha, J.-H., Rehemtulla, A., Ahn, B.-C., Jeon, Y.-H., Lee, J. Evaluation of therapeutic effects of natural killer (NK) cell-based immunotherapy in mice using *in vivo* apoptosis bioimaging with a caspase-3 sensor. *FASEB J.* 28, 2932–2941 (2014). www.fasebj.org**

Key Words: glioma · molecular imaging · Renilla *luciferase*

Natural killer (NK) cells are cytotoxic lymphocytes that are critical to innate immunity (1, 2). The killing effects of NK cells are regulated by either activating receptors that identify ligands on target cancer cells or by inhibitory receptors specific for major histocompatibility complex (MHC) class I molecules on cancer cells. They play an important role in eliminating target cells by 2 major mechanisms: perforin/granzymes and aggregation of target cell death receptors [Fas ligand-(FasL) or tumor necrosis factor-related apoptosis-inducing ligand (TRAIL)-related receptor; refs. 3–5]. A combination of perforin and granzyme leads to the intrinsic apoptosis pathway, which includes sequential molecular events such as the release of cytochrome *c*, formation of the apoptosome, and activation of effector caspase-3, -6, and -7. In addition, death receptor-mediated apoptosis leads to cell death through the extrinsic apoptosis pathway, resulting in activation of Bid and caspase-8 and -3 and, finally, execution of cell death.

The efficacy of NK-based immunotherapy has been reported to be dependent on the ability to manipulate the balance of activating/inhibitory receptors on NK cells and their cognate ligands, as well as the sensitivity of tumor cells to apoptosis (5–7). Although many studies have explored their efficacy in anticancer therapy, no clear clinical benefit has been demonstrated due to several factors, such as alteration of NK cell functions, chronic inflammation, regulatory T cell hindrance, and cytokine imbalance (8). Therefore, a better understanding of the mechanisms leading to NK

Abbreviations: Ab, antibody; BLI, bioluminescence imaging; DC, dendritic cell; DEVD, aspartic acid-glutamine-valine-aspartic acid; FasL, Fas ligand; FRET, fluorescent resonance energy transfer; IFN-γ, interferon; MHC, major histocompatibility complex; NK, natural killer; PARP, poly(ADP-ribose) polymerase; PBS, phosphate-buffered saline; PI3K, phosphatidylinositol 3-kinase; PMA, phorbol 12-myristate 13-acetate; Rluc, *Renilla* luciferase; T:E, target/effector; TNF, tumor necrosis factor; TRAIL, tumor necrosis factor-related apoptosis-inducing ligand

[1] Correspondence: Y.H.J., Leading-Edge Research Center for Drug Discovery and Development for Diabetes and Metabolic Disease, Kyungpook National University Hospital, 807 Hogukro, Bukgu, Daegu, 702-210, South Korea. E-mail: jeon9014@gmail.com; J.L., Department of Nuclear Medicine, Kyungpook National University Hospital, 50 Samduk 2-ga, Daegu, 700-721, South Korea. E-mail: jaetae@knu.ac.kr

doi: 10.1096/fj.13-243014

This article includes supplemental data. Please visit *http://www.fasebj.org* to obtain this information.

0892-6638/14/0028-2932 © FASEB

therapy failure is required for the development of novel treatment paradigms to improve therapeutic outcome.

NK cell-mediated death is involved in multiple apoptosis pathways, including intrinsic and extrinsic apoptosis. Although a number of specific assays to detect apoptosis progression have been developed, all assays developed to date, including assays based on caspase activation by a fluorescent substrate, fluorescent resonance energy transfer (FRET) construct-based assays, phosphatidyl serine exposure assays, assays that detect DNA-strand breaks, vital dye-based assays (calcein-AM), and radioprobe-based assays, measure apoptosis progression based on single-endpoint determinations (9). These methods determine the level of apoptosis *in vitro* and are not amenable to use in animal models, which hinders comprehensive understanding of the failure of NK cell therapy. Thus, the development of methods that can be used in real time is needed for the precise identification of apoptotic events.

Specialized molecular imaging tools that can reveal dynamic processes of apoptosis activation may provide the deconvolution of apoptosis-related biochemical cascades, as well as allow for a better understanding of the combination of various therapeutic modalities with NK-cell based therapy. Furthermore, this imaging platform may facilitate the evaluation of several important factors, such as the determination of effector/target ratio, cytotoxictiy, adjuvant supplement, and *in vivo* therapeutic protocol. Noninvasive imaging of apoptosis induced by treatment with certain chemotherapeutic drugs was successfully undertaken in a human glioma cancer model using a reporter for caspase-3 proteolysis (10). Based on our recent work, we postulate that caspase-3-dependent apoptosis activation generated by NK cell cytotoxicity could also be serially monitored by a caspase-3 biosensor in living animals noninvasively, and this system would be very helpful in the preparation of a preclinical setting of cell therapy.

In this study, we monitored the activation of caspase-3-dependent apoptosis by NK cell-based immunotherapy in an animal model of human glioma cancer expressing a caspase-3 sensor and renilla luciferase *in vitro* and *in vivo*. A molecular bioluminescence imaging (BLI) approach was undertaken in an effort to more objectively delineate the response of NK-cell based therapy through 2 different reporters, in which BLI of the caspase-3 sensor is used to monitor apoptosis by measuring caspase-3-linked activation and BLI of the *Renilla* luciferase (*Rluc*) gene is used to measure cell viability.

MATERIALS AND METHODS

Animals

Pathogen-free 6-wk-old female Balb/c nude mice were obtained from SLC (Shizuoka, Japan). All animal experimental protocols were approved by the Committee for the Handling and Use of Animals of Kyungpook National University.

Cell lines

NK92 cells (human IL-2-dependent NK cells) to be used as effectors were purchased from American Type Culture Collection (ATCC; Manassas, VA, USA) and maintained in α minimum essential medium without ribonucleosides and deoxyribonucleosides and supplemented with 2 mM L-glutamine, 1.5 mg/ml sodium bicarbonate, 0.2 mM inositol, 0.1 mM 2-mercaptoethanol, 0.02 mM folic acid, 12.5% horse serum, and 12.5% fetal bovine serum (Hyclone, Logan, UT, USA) at 37°C in a 5% CO_2 atmosphere.

D54 human glioma cells were cultured in RPMI 1640 medium supplemented with 10% fetal bovine serum (Hyclone), 1% antibiotic-antimycotic (Gibco, Grand Island, NY, USA), and GlutaMAX (Gibco) at 37°C in a 5% CO_2 atmosphere.

The MDA-MB-231-derived human breast cancer cell line 1833 was cultured in DMEM supplemented with 10% fetal bovine serum, 1% antibiotic-antimycotic, and GlutaMAX at 37°C in a 5% CO_2 atmosphere.

D54 and 1833 cells were transfected with the caspase-3 sensor construct using Fugene 6 (Roche, Aurora, OH, USA), and stable clones were selected with G418 (Gibco). D54 and 1833 cells that stably expressed the caspase-3 sensor were further transduced with lentivirus coexpressing *Rluc*, mcherry, and puromycin genes under the control of CMV promoter (Genecopoeia, Rockville, MD, USA). Stable clones were selected with puromycin (Sigma-Aldrich, St. Louis, MO, USA). The established stable cell lines expressing both the caspase-3 sensor and *Rluc* gene are herein referred to as D54-CR and 1833-CR cells, respectively.

In vitro bioluminescence imaging

To evaluate apoptosis induction in the stable clones (D54-CR and 1833-CR cells) by NK92 cells, effector and target cells were cocultured with growth medium containing 1% Glosensor (Promega, Madison, WI, USA) at different target/effector (T:E) ratios in white and clear bottom 96-well plates, and BLI signals were measured at the indicated times using a microplate reader.

For the inhibition studies of caspase-3 activation, D54-CR cells were plated in white and clear bottom 96-well plates. After 24 h, the medium was replaced with growth medium containing 1% Glosensor (Promega). Vehicle, Z-VAD-FMK (a pan-caspase inhibitor, drug concentration 200 μM; Tocris, Bristol, UK), PD98059 (ERK inhibitor, 10 μM; Sigma-Aldrich), and wortmanin [phosphatidylinositol 3-kinase (PI3K) inhibitor, 10 μM; Sigma-Aldrich] were added to each well for 2 h. NK92 cells were cocultured with D54-CR cells at a T:E ratio of 1:5, and BLI activity was measured using a microplate reader at the indicated times.

To monitor caspase-3 activation by stimulated or nonstimulated NK92 cells, NK92 cells were treated with or without a combination of phorbol 12-myristate 13-acetate (PMA, 10 ng/ml; Sigma-Aldrich) and ionomycin (1 mg/ml; Sigma-Aldrich) for 2h. Stimulated and nonstimulated-NK92 cells were coincubated with D54-CR cells at a T:E ratio of 1:2.5, and BLI activity was measured using a microplate reader at the indicated times.

FACS analysis

D54-CR cells were plated in 6-well plates and incubated with rTRAIL (90, 180, 360, and 720 ng/ml) for 6 h. After 24 h, the cells were trypsinzed and collected by centrifugation. PE-conjugated cleaved caspase-3 Ab (BD Biosciences, San Jose, CA, USA) was added to each plate, and caspase-3-positive cells

were determined using a BD FACSCanto flow cytometer (BD Biosciences).

To determine the fraction of cleaved caspase-3-positive cells or annexin-V-positive cells in the D54-CR tumors treated with either phosphate-buffered saline (PBS) or NK92 cells, mice were killed and the tumor masses were extracted. Tumors were dissociated using collagenase D (Roche), and single cells were stained with either Alexa Fluor 647-conjugated cleaved caspase-3 Ab or FITC-conjugated annexin V Ab (BD Biosciences). Flow cytometric analysis was performed using a BD FACScan unit using CellQuest software (BD Immunocytometry Systems; BD Biosciences).

Western blot

Parental cells or established stable clones (1833, 1833-CR, D54, and D54-CR cells) were washed in PBS and lysed with RIPA buffer (Invitrogen, Carlsbad, CA, USA) including complete protease inhibitor cocktail (Roche). The protein concentration was estimated using a bicinchoninic acid (BCA) kit (Pierce, Rockford, IL, USA). The media and lysates were separated by SDS-PAGE, and protein expression was detected by Western blot analysis using antibodies (Abs). Equal amounts of protein were loaded in each lane and resolved by 4–12% gradient Bis-Tris gel (Invitrogen). Proteins were transferred to 0.2 μm polyvinylidene difluoride (PVDF) membrane (Invitrogen). Membranes were blocked and incubated overnight at 4°C with primary Abs and then incubated with the appropriate horseradish peroxidase (HRP)-conjugated secondary antibody at room temperature for 1 h. ECL-Plus (Amersham Pharmacia, Uppsala, Sweden) was used to detect peroxidase activity according to the manufacturer's protocol. Abs raised against luciferase, caspase-3, poly(ADP-ribose) polymerase (PARP), and β-actin were purchased from Cell Signaling Technology (Beverly, MA, USA).

In vivo NK therapy

D54-CR cells (5×10^6) were subcutaneously implanted into the right hind flanks of nude mice ($n=30$). When tumor formation was detected, the mice were divided into 3 groups: a control group for PBS treatment and 2 therapy groups for NK92 cell (2×10^6 and 1×10^7 cells/mouse, respectively) treatment. After injection, BLI was acquired to monitor caspase-3 activation as well as *Rluc* gene for therapeutic response at the indicated times.

BLI of the caspase-3 sensor and *Rluc* gene was obtained using an IVIS Lumina II (Perkin-Elmer, Wellesley, MA, USA) immediately before injection and 12, 24, and 48 h after administration of NK92 cells. Mice received a single dose of substrate for each reporter (D-luciferin or coelentrazine, 3 mg/mouse or 15 μg/mouse, respectively; Perkin-Elmer) when BLI was performed at each time point. Mice were anesthetized with a 1–2% isofluorane/air mixture, and serial images were acquired over 20–30 min to capture the peak photon emission for each animal. Regions of interest were drawn around the area of interest in each mouse, and peak luminescence values of each series were used for analysis. The fold increase of induction for the caspase-3 sensor was calculated by dividing the BLI activity of the caspase-3 sensor (cellular apoptosis) by the BLI activity of *Rluc* gene (cell viability) at each time point.

Statistical analysis

All data are expressed as means ± SD, and statistical significance was determined using an unpaired Student's test. The statistical significance and the error bars for FACS analysis were determined using ANOVA, which determines the mean differences between each group. Values of $P < 0.05$ were considered statistically significant.

RESULTS

Establishment of reporter tumor cells for both caspase-3 activation and cellular viability

For monitoring caspase-3 activation and the therapeutic response of target cancer cells to NK therapy, we successfully established stable cell lines expressing 2 reporters; a caspase-3 sensor construct as a caspase-3 proteolysis marker and the renilla luciferase gene as a surrogate marker of cell viability. Western blot analysis using anti-luciferase Ab showed luciferase protein for caspase-3 sensor (~69.3 kDa) in D54-CR and 1833-CR cells but not parental cells (Supplemental Fig. S1*A*). The BLI signal of the R*luc* gene was increased in a cell number-dependent manner in D54-CR and 1833-CR cells but not in either line of parent cells ($R^2=0.86$ and $R^2=0.92$, D54-CR and 1833-CR, respectively; Supplemental Fig. S1*B*, *C*).

Treatment of D54-CR and 1833-CR cells with rTRAIL resulted in a time- and dose-dependent increase in BLI activity compared with cells subjected to PBS treatment (Supplemental Fig. S1*D*, *E*).

As shown in Supplemental Fig. S1*F*, the percentages of cleaved caspase-3-positive cells increased according to TRAIL dose (1-way ANOVA, $P<0.0001$), revealing a good correlation between caspase-3 activation and the level of cleaved caspase-3 ($R^2=0.95$; Supplemental Fig. S1*G*).

Monitoring of caspase-3 activation by NK92 cell cytotoxicity *in vitro*

To demonstrate caspase-3 activation by the therapeutic effects of NK92 cells *in vitro*, NK92 cells were incubated with D54-CR and 1833-CR cells at T:E ratios of 1:2.5, 1:5, and 1:10, and BLI signals were measured. Incubation of D54-CR cells with NK92 cells led to a time- and dose-dependent increase in BLI activity compared with cells treated with PBS (**Fig. 1*A*, *B***); peak activity in the BLI signal of the caspase-3 sensor at all T:E ratio was measured 4 h post-treatment. Consistent with the increase in BLI activity of the caspase-3 sensor, Western blot analysis of D54-CR cells also revealed increases in cleaved PARP protein in a dose-dependent manner (Fig. 1*C*) and subsequently showed a time-dependent increase in caspase-3 activation as measured by cleavage of capsase-3 and PARP (Fig. 1*D*).

Interestingly, the caspase-3 sensor showed the different susceptibility of breast and glioma cancer cells to NK92 cells *in vitro*. As illustrated in Fig. 1*E*, the susceptibility of D54-CR cells to NK92 cells was higher than that of 1833-CR cells, resulting in a peak in BLI activity at 4 h post-treatment (D54-CR cells and 1833-CR cells, ~24.6 and ~6.6-fold induction, respectively).

Inhibition studies were performed to examine the selectivity of the caspase-3 sensor using Z-VAD-FMK, wortmannin, and PD98059, and the following results were obtained. First, treatment with NK92 resulted in an ~18.5-

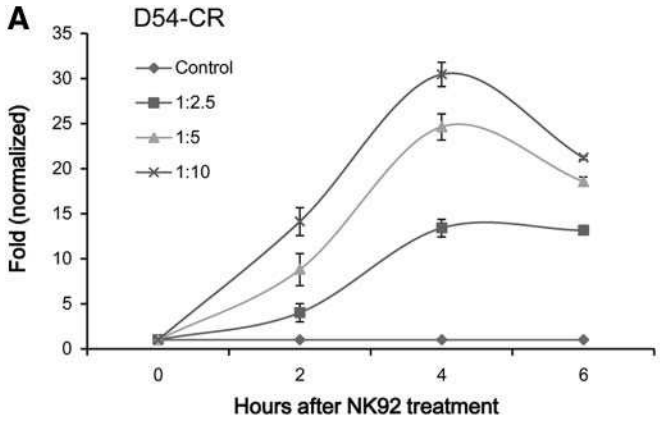

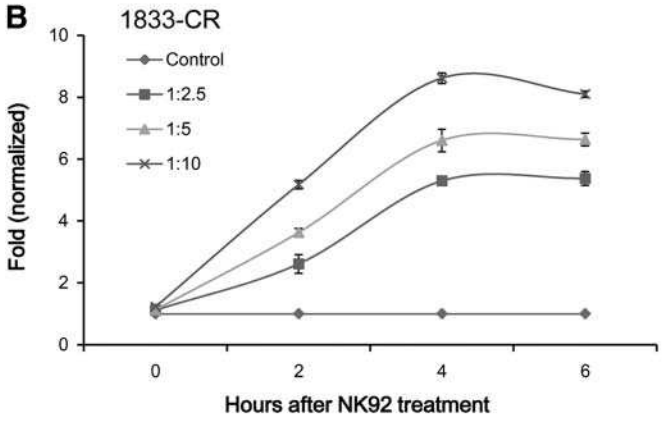

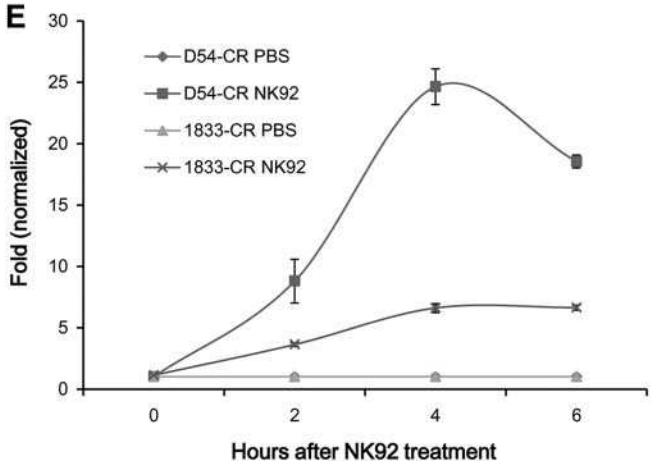

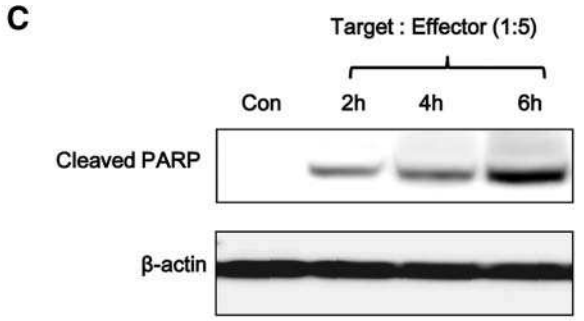

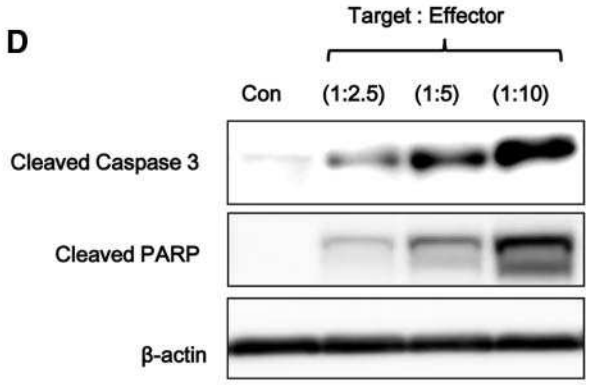

Figure 1. Change in caspase-3 sensor activity by *in vitro* treatment of NK92 cells. *A*, *B*) Increase in caspase-3 sensor activity following NK92 treatment. Stable D54-CR (*A*) and 1833-CR (*B*) clones were plated in 96-well plates, and NK92 cells were added to each well at a different T:E ratio; BLI activity (caspase-3 sensor and *Rluc* gene) was then measured at every hour for 6 h. *C*, *D*) Representative Western blots of lysates from NK92-treated D54-CR cells using anti-cleaved PARP (*C*, *D*) and caspase-3 (*D*) Abs. D54-CR cells were treated with NK92 cells, and cell lysates were prepared for Western blot analysis. Lysates were probed with β-actin Ab to control for loading. *E*) Varying susceptibility of stable clones (D54-CR and 1833-CR) against NK92 killing. Stable clones of D54-CR and 1833-CR cells were plated in 96-well plates, and effector was added to target cells 24 h later at a T:E ratio of 1:5. BLI activity for the caspase-3 sensor or *Rluc* gene was measured and plotted as fold induction over values obtained from vehicle-treated cells. BLI activity of the caspase-3 sensor was normalized with that of the *Rluc* gene. Experiments were performed at least in triplicate; values are means ± SD.

fold induction in BLI activity 5 h after NK92 treatment to D54-CR cells compared with vehicle treatment, while BLI activity (showing the caspase-3 activation) in cancer cells treated with NK92 was almost completely blocked by Z-VAD-FMK (**Fig. 2*A***). Caspase-3 activation was not detected in D54-CR cells incubated with either vehicle or Z-VAD-FMK alone. Second, treatment of wortmannin led to decreases in BLI activity in D54-CR cells incubated with NK92 cells, while NK92 treatment resulted in a ~19.4-fold increase in BLI activity compared with cells treated with vehicle only (Fig. 2*B*). Treatment with PD98059 also resulted in a drastic decrease in BLI activity in D54-CR cells treated with NK92 cells; an ~19.2-fold increase in BLI activity in D54-CR cells was observed following NK92 treatment (Fig. 2*C*).

We evaluated whether the caspase-3 sensor could show modulated cytotoxicity when NK92 cells were stimulated with specific agents such PMA and ionomycin, leading to promotion of cytokine secretion [tumor necrosis factor (TNF) and interferon γ (IFN-γ)]. Stimulation of NK92 cells resulted in a more rapid and higher fold induction in BLI activity of the caspase-3 sensor in D54-CR cells compared with nonstimulated NK92 cells (Fig. 2*D*).

In vivo imaging of capsase-3 activation following adoptive transfer of NK92 cells to D54-CR tumor model and evaluation of its antitumor effects

Adoptive transfer of either PBS or NK92 cells in D54 tumor-bearing mice resulted in an increase in BLI

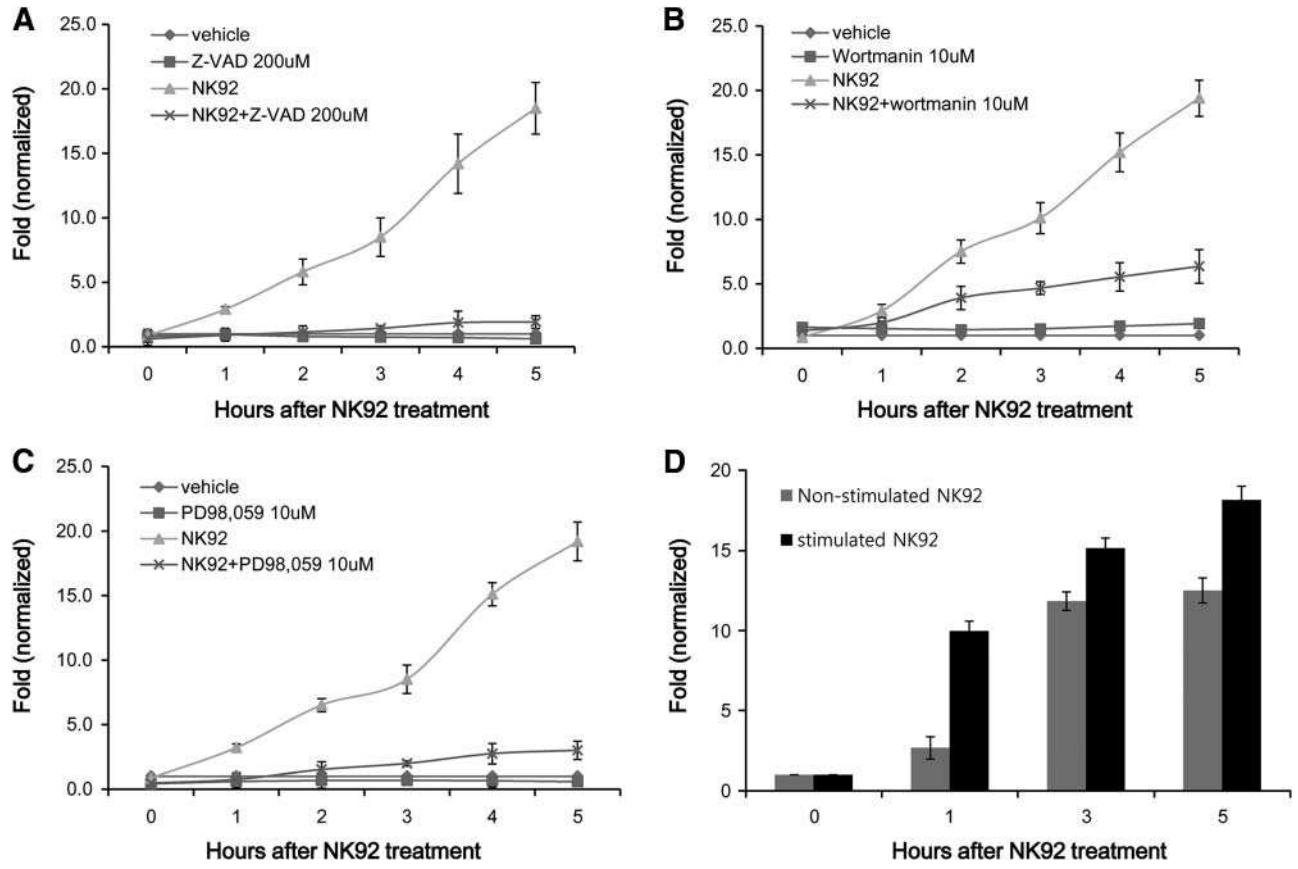

Figure 2. Measurement of selectivity of NK92-mediated killing against target cells with caspase-3 sensor. *A–C*) Inhibition of caspase-3 sensor activity by treatment with Z-VAD (*A*), wortmanin (*B*), and PD 98059 (*C*), which block the signaling pathways leading to apoptosis and cytotoxicity. D54-CR cells were plated in 96-well plates, and the indicated compounds were added to target cells for 1 h. Then, NK92 cells were added to the target cells at a T:E ratio of 1:5. BLI activity of the caspase-3 sensor or *Rluc* gene was measured. *D*) Enhanced cytotoxicity of NK92 cells by combined treatment of PMA and ionomycin. NK92 cells were treated with or without a combination of PMA and ionomycin for 2 h. Nonstimulated and stimulated NK92 cells were coincubated with D54-CR cells at T:E ratio of 1:2.5, and BLI activity (caspase-3 sensor and *Rluc* gene) was measured every hour for 5 h. BLI activity was plotted as fold induction over the values obtained from vehicle treated cells. BLI activity of the caspase-3 sensor was normalized with that of R*luc* gene. Experiments were performed at least in triplicate; values are means ± SD.

activity of the caspase-3 sensor depending on the number of administered effectors when images were acquired at the indicated times (**Fig. 3*A, B***). Differences in BLI activity of the *Rluc* gene were not detected between the PBS treatment group and the NK92 treatment group 24 h post-treatment (data not shown). FACS analysis of the excised tumors with anti-cleaved caspase-3 Ab revealed an increase in cleaved caspase-3 levels in tumors treated with NK92 cells compared with those treated with PBS, showing an increase in active caspase-3-positive cells by increasing the number of effector cells (Fig. 3*C*).

Antitumor effects induced by NK-based immunotherapy were also monitored in D54-CR tumor-bearing mice by evaluating the level of caspase-3 activation using the caspase-3 sensor, as depicted in Supplemental Fig. S2. The BLI activity of the caspase-3 sensor from tumors was not increased in mice treated with PBS. However, adoptive transfer of NK92 cells to D54-CR tumor-bearing mice resulted in an increase in the BLI activity of the caspase-3 sensor immediately after treatment (**Fig. 4*A, B***). Particularly, repeated treatment with NK92 cells resulted in an increase in the cumulative BLI activity of the caspase-3 sensor until d 15, after which time BLI activity declined. Treatment with a higher number of NK92 cells (1×10^7 cells) resulted in greater increases in BLI activity of the caspase-3 sensor from tumors compared with mice treated with lower numbers of NK92 cells (2×10^6 cells). Mice receiving either 2×10^6 or 1×10^7 NK92 cells had an ~12.5 and ~18.2 maximum fold increase in BLI activity of the caspase-3 sensor, whereas PBS-treated mice had a minimal increase in BLI activity of the caspase-3 sensor.

When the peak activity of the caspase-3 sensor was detected at d 15, tumors were excised, and single cells were isolated to further determine levels of both cleaved capsase-3 and annexin-V in tumors from mice receiving either PBS or varying numbers of NK92 cells. FACS analysis demonstrated that tumors from NK92-treated mice showed an increase in active capsase-3 levels in an NK92 cell number-dependent manner compared with those from PBS-treated mice (Fig. 4*C*). Consistent with the cleaved caspase-3 results, apoptosis analysis with anti-annexin V Ab demonstrated that the increase in annexin-V levels in tumors from mice

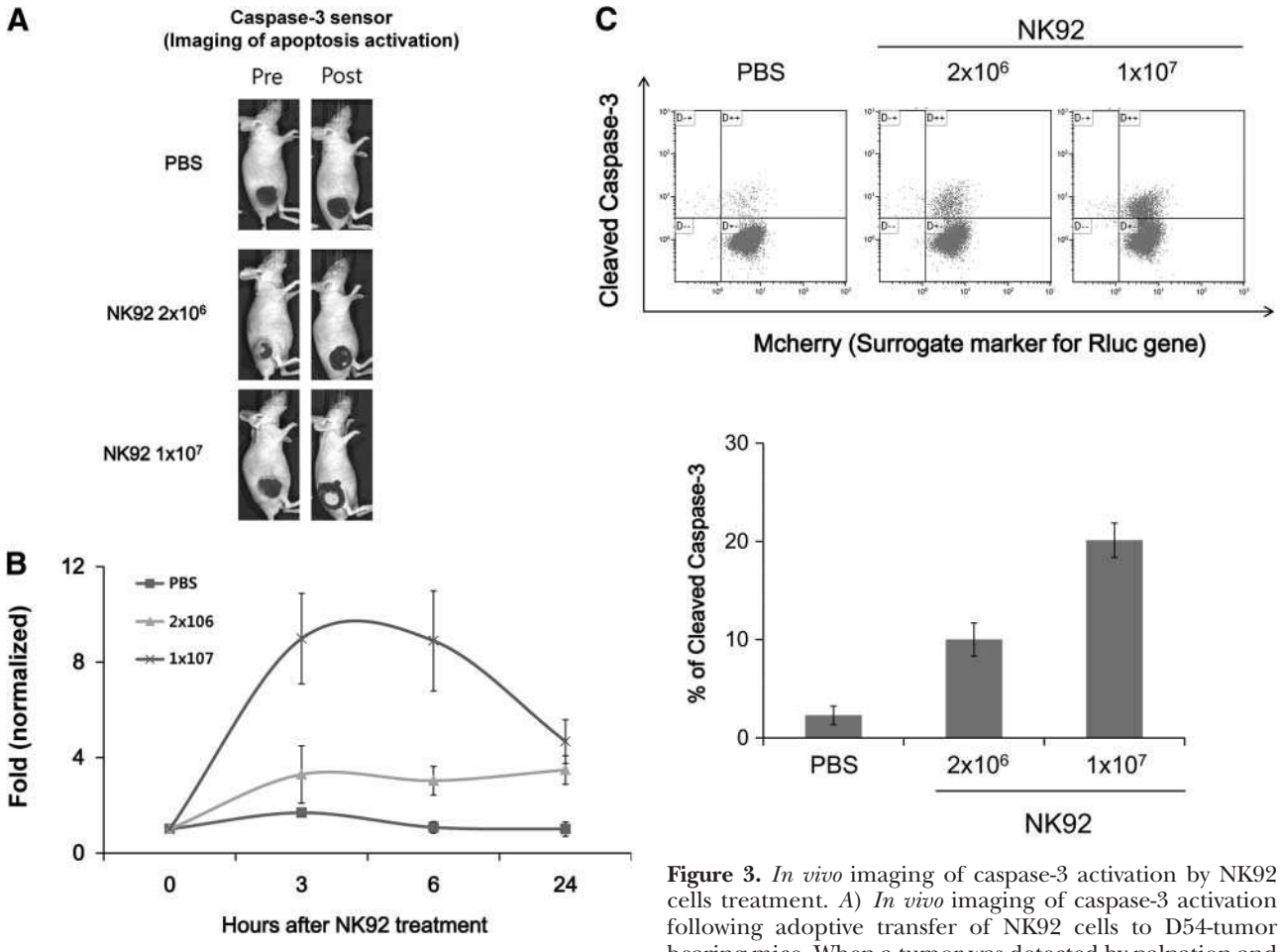

Figure 3. *In vivo* imaging of caspase-3 activation by NK92 cells treatment. *A*) *In vivo* imaging of caspase-3 activation following adoptive transfer of NK92 cells to D54-tumor bearing mice. When a tumor was detected by palpation and inspection, NK92 cells (2×10^6 or 1×10^7 cells/mouse) were transfused to tumor-bearing mice, and BLI was acquired at the indicated time. *B*) Quantification of caspase-3 activation. *C*) FACS analysis to evaluate both cleaved caspase-3 and annexin V levels. At the end of the animal study, tumors were excised and further processed for FACS analysis. Either the cleaved caspase-3 or apoptosis level was determined in isolated cells from the tumor tissue of mice receiving either PBS or NK92 at different T:E ratios with anticleaved caspase-3 Ab. Mcherry fluorescent protein is the surrogate marker for *Rluc* gene. Bars represent percentage of cleaved caspase-3-positive cells. BLI activity was plotted as fold induction over values obtained from vehicle-treated cells. BLI activity of the caspase-3 sensor was normalized with that of the *Rluc* gene. Experiments were performed at least in triplicate; values are means ± SD.

receiving NK92 cells was proportional to the number of infused NK92 cells (Fig. 4*D*).

In vivo imaging of tumors using a R*luc* reporter gene revealed that treatment with lower numbers of NK92 cells resulted in moderate retardation of tumor growth compared with the PBS-treated group. Particularly, mice treated with high doses of NK92 cells exhibited marked retardation of tumor growth compared with mice treated with low doses of NK92 cells. At d 18 after treatment, PBS-treated mice exhibited a 170% increase in BLI activity, whereas mice treated with a lower or higher dose of NK92 cells showed an increase of 49 and 4.9% in BLI activity, respectively (**Fig. 5**). When tumor volume was measured with calipers, a delay in tumor growth was observed in the NK92 treated group but not in the PBS-treated group from d 4 until d 18 after *in vivo* therapy, which is consistent with the results of *in vivo* BLI of the *Rluc* gene (Supplemental Fig. S3). However, inhibition of tumor growth was not observed in the PBS treated group during *in vivo* therapy.

DISCUSSION

Intense attention has been given to NK cell-based immunotherapy as a potentially effective therapeutic tool, because of its selective killing effect against cancer cells (11). Recently, a number of clinical approaches have been used to evaluate the possibility of NK therapy in a variety of cancers. However, it has been difficult to achieve promising outcomes in clinical cases because of the unsuitable ratio of effector to target cells, weak cytotoxicity, tumor targeting of an insufficient number of effectors, and hindrance of immuomodulatory cytokines or immune cells. Effective strategies for improving NK cell-based immunotherapy remain to be further investigated.

Serial molecular events related to apoptosis in cultured cells and/or animal tumor models induced by newly developed NK cell therapy have been evaluated with traditional immunological and biochemical techniques such as the ^{51}Cr release assay, lactate dehydro-

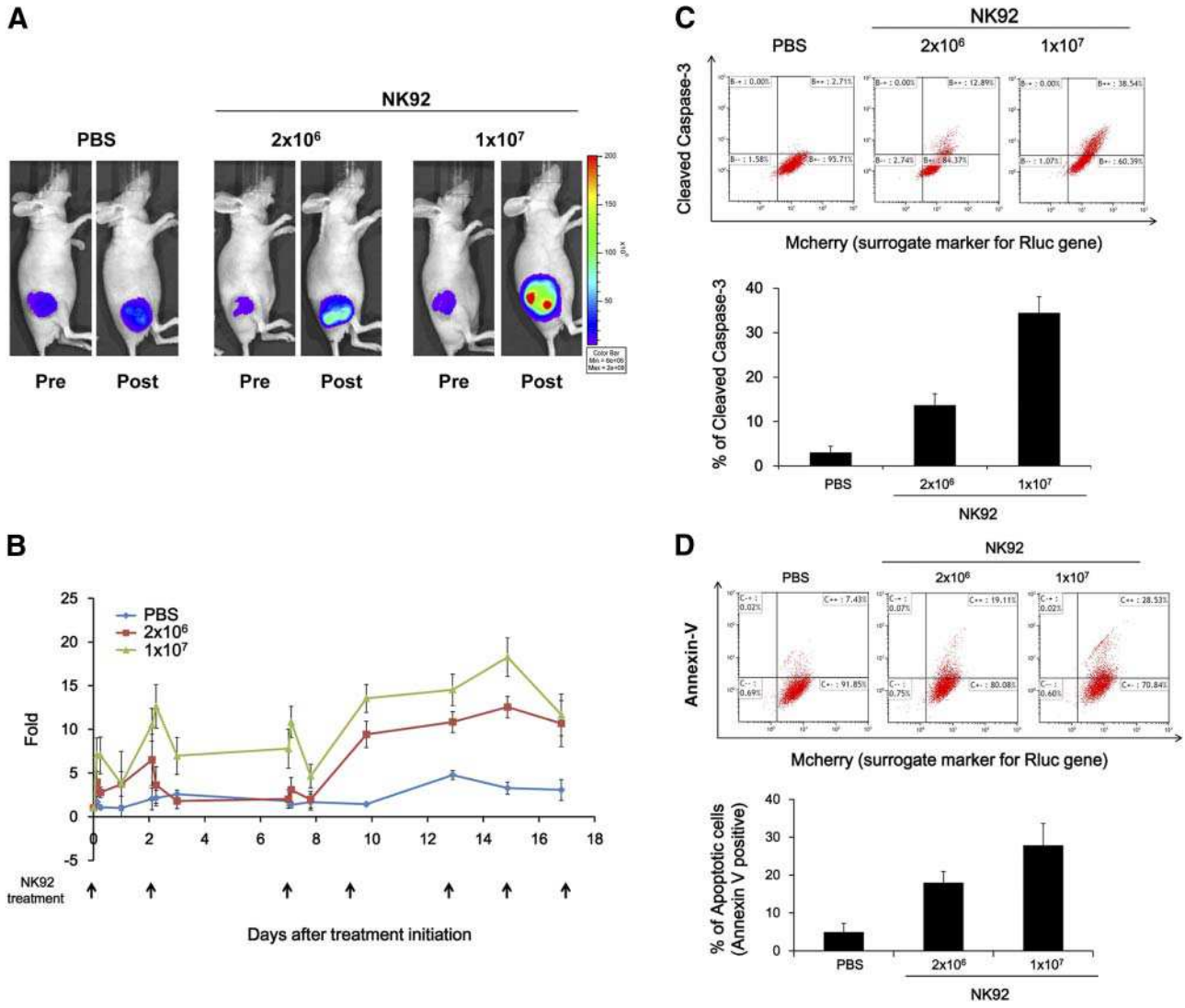

Figure 4. Application of caspase-3 sensor in experimental setting of NK-based immunotherapy. *A*) Representative BLI (showing the maximum caspase-3 activation) from D54-CR tumor-bearing mice before and after treatment with NK92 cells. When a tumor was detected by palpation and inspection, NK92 cells (2×10^6 or 1×10^7 cells/mouse) were intravenously transferred to tumor-bearing mice at the indicated time, and BLI was acquired. *B*) Quantification of caspase-3 activation. BLI activity was plotted as fold induction over values obtained from vehicle-treated cells. BLI activity of the caspase-3 sensor was normalized with that of R*luc* gene. *C*, *D*) FACS analysis to evaluate either the cleaved caspase-3 (*C*) or annexin-V (*D*) level. At the end of the animal study, tumors were excised and further processed for FACS analysis. Either cleaved caspase-3 or apoptosis levels were determined in isolated cells from the excised tumor tissue of mice receiving either PBS or NK92 cells at different T:E ratios with anti-cleaved caspase-3 or annexin V Abs. Mcherry fluorescent protein is the surrogate marker for *Rluc* gene. Bars represent percentage cleaved caspase-3- or annexin-V-positive cells. Experiments were performed at least in triplicate; values are means ± SD.

genase (LDH) assay, flow cytometry, and protein-based assays such as Western blotting. These analytical tools only allow a nonquantitative snapshot of the interactive cascade of signaling events following therapeutic intervention and can overlook the time-and dose-dependent molecular effects during evaluation of NK cytotoxicity. Thus, innovative imaging tools are needed to enable real-time monitoring of the sequential cellular events of apoptosis induced by cell therapies such as NK-based immunotherapy.

The present study utilized a genetically engineered caspase-3 sensor for the dynamic and quantitative imaging of apoptotic molecular events in living animals. We previously reported a caspase-3 biosensor based on a split luciferase system (10). This apoptosis sensor is made of the split luciferase domains fused to interacting peptides, pepA and pepB, with an intervening caspase-3 cleavage motif [aspartic acid-glutamine-valine-aspartic acid (DEVD) sequence]. On induction of apoptosis, this sensor is proteolytically cleaved by caspase-3 at the DEVD motif, and this cleavage induces the reconstitution of luciferase activity through the interaction of NLuc and CLuc. Here, we attempted to not only monitor the activation of apoptosis induced by NK therapy in a glioma cancer model *in vitro* and *in vivo* using a caspase-3 sensor but also evaluate the therapeutic effects of NK therapy using a *Rluc* reporter gene system.

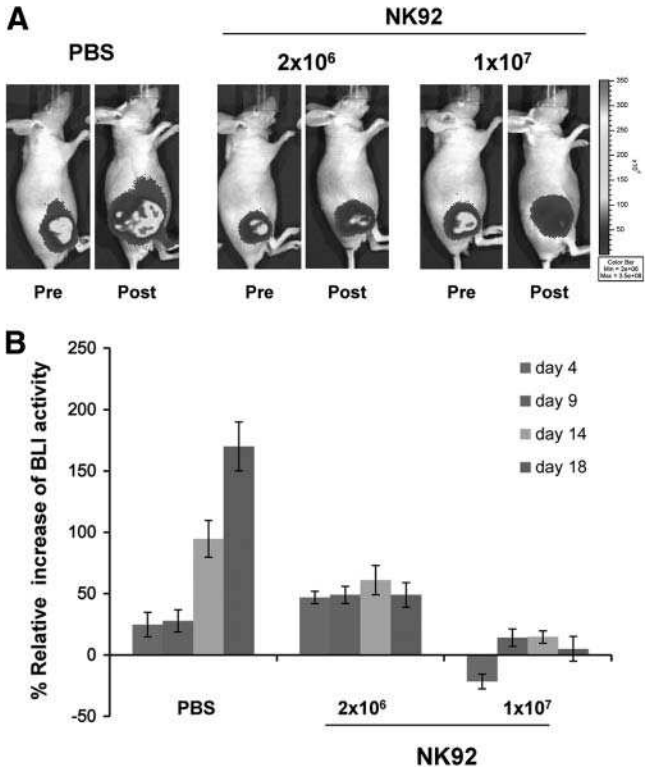

Figure 5. *In vivo* monitoring of antitumor effects of NK therapy by optical imaging using the *Rluc* reporter gene. *A*) Monitoring the antitumor effects by NK-based immunotherapy. BLI activity was measured at the indicated times to monitor tumor progression. *B*) Quantification of BLI activity in the *Rluc* reporter gene. BLI was obtained on initiation of NK92 cell therapy at the indicated times, and regions of interest analysis of BLI activity in the tumors was performed to evaluate the therapeutic response of NK92 therapy. Bars represent relative change in BLI activity of the treatment group compared with the control group. Experiments were performed at least in triplicate, values are means ± SD.

NK92 cells (IL-2-dependent and highly activated NK cells) were adopted as an effector in the current study because NK92 cells are reported to have high killing effects against various cancer cells, including myeloma, leukemia, malignant lymphoma, melanoma, ovarian, bladder, and breast cancer, in preclinical or clinical settings (12, 13), and they are easy to handle with simple supplementation of IL-2. Breast and glioma cancer cells expressing a caspase-3 sensor construct were established as target cells. An *Rluc* reporter gene was further transduced in target cells using a lentiviral system because it enables quantification of cellular viability, which is an important factor in apoptosis-related studies. Thus, stable cells expressing both a caspase-3 sensor and an *Rluc* gene may be able to simultaneously detect caspase-3 activation as well as determine cellular viability after NK92 treatment.

Several studies have demonstrated that TRAIL induces extrinsic apoptosis by binding death receptor (DR4/5) and activates effector caspase-3 (14–16). Using rTRAIL, we also confirmed that the functional activity of the caspase-3 sensor after rTRAIL treatment of stable clones of D54-CR and 1833-CR is increased, as shown by increased BLI activity in caspase-3 sensor in a dose- and time-dependent manner. FACS analysis with anti-cleaved caspase-3 Ab also demonstrated the increase in cleaved caspase-3 levels in rTRAIL-treated D54-CR cells in a dose-dependent manner; a good correlation was observed between caspase-3 activation and the level of cleaved caspase-3. Furthermore, the BLI activity of *Rluc* showed a decrease in cell viability in the same manner. These findings suggest that the BLI activity of the caspase-3 sensor is representative of the level of caspase-3 activation that occurs in cancer cells even before cell death by treatment with immune effector cells.

In accordance with our rTRAIL experiment data, treatment of NK92 cells resulted in an increase in the BLI activity of the caspase-3 sensor in a time- and dose-dependent manner *in vitro*. These findings are consistent with the results of the Western blot analysis for caspase-3 activity, as determined by both cleavage caspase-3 and PARP Ab. Furthermore, we determined the selectivity of the caspase-3 sensor in NK-mediated apoptosis with specific apoptosis inhibitors. Treatment of NK92 cells resulted in strong BLI activity in D54-CR cells, but caspase-3 activation was effectively inhibited with three different inhibitors (Z-VAD, wortmannin, and PD98059). These compounds are well known to inhibit sequential signaling events, such as caspase, PI3K, and extracellular signal-regulated kinase (Erk), which are associated with the activation of apoptosis induced by NK cell-mediated cytotoxictiy. These findings suggest that specific cellular signaling events related to caspase-3 activation generated by NK cell cytotoxicity can be monitored in live cells, which is essential for the optimization of NK cell-based therapy.

Improving NK-mediated cytotoxicity by modulating effector cells with cytokine genes and chemical compounds such as PMA and ionomycin is an essential element to achieving more successful therapeutic effects before adoptive transfer of NK cells *in vivo* (17–20). It was reported that the combination of the protein kinase activator PMA and the ionomycin increased robust secretion of the cytokines TNF and IFN-γ and resulted in accelerated cellular apoptosis (21, 22). In our *in vitro* study of applying PMA/ionomycin to NK92 cells, we also observed a more rapid increase and higher levels of the BLI signals of the caspase-3 sensor following stimulation of NK92 cells with 2 compounds. Moreover, we observed different susceptibilities to NK92 cell therapy between breast cancer cells (1833-CR) and glioma cancer cells (D54-CR) using the caspase-3 sensor. These findings should be an important issue when designing the tailored strategies of NK-based therapy. For example, when breast cancer cells are not susceptible to NK cells during early screening of NK cell cytotoxicity against cancer cells, a combination of NK therapy and other therapeutic strategies such as radiation and chemotherapy, which has reported to modulate the phenotype marker of cancer cells as well as increase the susceptibility of target cells (23–27), could be considered. If combinations of different methods with NK cells could be properly selected for breast cancer cells, increases in the BLI signals of the caspase-3 sensor would be greater after combination treatment.

D54-CR cells were used for the target animal tumor model in our *in vivo* study because D54 target cells were shown to be more susceptible to NK92 therapy than 1833 breast cancer cells as depicted in Fig. 1*E*. *In vivo* caspase-3 activation was noninvasively monitored following an adoptive transfer of different doses of NK92 cells to D54-CR tumor bearing mice. Increase in the BLI signal of the caspase-3 sensor was observed in an effector number- and time-dependent manner, which is consistent with an increase in cleaved caspase-3 levels in isolated cells from tumor tissues. Normally, we can observe the peak BLI activity (showing the caspase-3 activation) in tumors of treated mice at 3 h after injection. Although the migration of infused NK cells was not monitored using an *in vivo* imaging modality, we can presume that infused NK92 cells may localize to the tumor site at early time points (within 3 h) and attack and kill target cells, resulting in an increase in caspase-3 BLI activity and a decrease in *Rluc* activity. These findings are also consistent with the report of Melder *et al.* (28), in which animal PET imaging with ^{11}C methyl iodide was used for successful monitoring of the migration of NK cells in tumor-bearing mice. Localization of labeled NK cells in tumor vasculature was observed at 30 min to 1 h postinjection in their study.

For an *in vivo* setting of NK cell therapy, as shown in Fig. 5*A*, repeated transfusion of either higher or lower numbers of NK92 cells resulted in a gradual increase in BLI activity of the caspase-3 sensor during the course of treatment, revealing that treatment with a higher dose of NK92 cells is more effective in the induction of caspase-3 dependent apoptosis than a lower dose. Furthermore, when tumor growth by NK92 therapy was serially monitored using the *Rluc* reporter gene, higher dose treatment was more effective for inhibition of tumor growth compared with lower dose treatment.

Based on the current results, we believe that the caspase-3 sensor could be extended to the DNA or dendritic cell (DC) vaccine-based immunotherapy field; DNA or DC vaccination leads to the tumor-specific immune response through antigen presentation of antigen-presenting cells (APCs) and subsequent stimulation of effectors [such as cytotoxic T cells (CTLs)] against cancer. Particularly, antitumor immunity is mainly dependent on successful activation and expansion of effector T cells, and thus, an imaging modality to noninvasively show the killing effects of effector T cells would be of considerable benefit for therapeutic setting optimization of DNA or DC-based immunotherapy.

There are some issues to address concerning the limitations of the current study. First, immunodeficient nude mice and the NK92 cell line were used to evaluate the therapeutic effects of NK-based immunotherapy; we adopted human cancer cells for the target because there are many different factors to be considered in the tumor microenvironment between immunodeficient and immunocompetent mouse systems. Thus, testing the potentials of caspase-3-sensor in immunocompetent mice with primary NK cells was required. Second, the caspase-3 sensor is based on a plasmid vector system, and the steps of transferring the sensor vector to target cells and selecting stable clones are undertaken during procedure. The original phenotype and character of cancer cells could be modified during the establishment of stable cell lines, which may affect the cytotoxicity of NK cells as an essential function of effectors. Thus, changes in the original character of cancer cell should be compared between parental cells and stable cells in a future study.

In summary, we successfully visualized cellular apoptotic events induced by NK cell therapy noninvasively both *in vitro* and *in vivo* using a caspase-3 biosensor. The BLI findings were well correlated with the antitumor effects of therapy *in vivo*. A molecular imaging technique with a caspase-3 sensor would facilitate preclinical evaluation of therapeutic protocols, including dosing, scheduling, and efficacy of NK-based immunotherapy. FJ

This work was supported by a Republic of Korea National Research Foundation (NRF) grant funded by the Ministry of Education, Science, and Technology (MEST; 2009-0078234), by the National Nuclear R&D Program through the NRF (MEST grant 2012M2A2A7014020), by the Repbulic of Korea Health Technology R&D Project, Ministry of Health and Welfare (grant A111345), by the Regional Technology Innovation Program of the Ministry of Knowledge Economy (MKE; grant RTI04-01-01), and by the Kyungpook National University Research Fund (2013).

REFERENCES

1. Cerwenka, A., and Lanier, L. L. (2001) Natural killer cells, viruses and cancer. *Nat. Rev. Immunol.* **1,** 41–49
2. Lanier, L. L. (2008) Evolutionary struggles between NK cells and viruses. *Nat. Rev. Immunol.* **8,** 259–268
3. Rosen, D., Li, J. H., Keidar, S., Markon, I., Orda, R., and Berke, G. (2000) Tumor immunity in perforin-deficient mice: a role for CD95 (Fas/APO-1). *J. Immunol.* **164,** 3229–3235
4. Trapani, J. A., and Smyth, M. J. (2002) Functional significance of the perforin/granzyme cell death pathway. *Nat. Rev. Immunol.* **2,** 735–747
5. Screpanti, V., Wallin, R. P., Grandien, A., and Ljunggren, H. G. (2005) Impact of FASL-induced apoptosis in the elimination of tumor cells by NK cells. *Mol. Immunol.* **42,** 495–499
6. McQueen, K. L., and Parham, P. (2002) Variable receptors controlling activation and inhibition of NK cells. *Curr. Opin. Immunol.* **14,** 615–621
7. Shi, J., Tricot, G. J., Garg, T. K., Malaviarachchi, P. A., Szmania, S. M., Kellum, R. E., Storrie, B., Mulder, A., Shaughnessy, J. D., Jr., Barlogie, B., and van Rhee, F. (2008) Bortezomib down-regulates the cell-surface expression of HLA class I and enhances natural killer cell-mediated lysis of myeloma. *Blood* **111,** 1309–1317
8. Zamai, L., Ponti, C., Mirandola, P., Gobbi, G., Papa, S., Galeotti, L., Cocco, L., and Vitale, M. (2007) NK cells and cancer. *J. Immunol.* **178,** 4011–4016
9. Kepp, O., Galluzzi, L., Lipinski, M., Yuan, J., and Kroemer, G. (2011) Cell death assays for drug discovery. *Nat. Rev. Drug Discov.* **10,** 221–237
10. Coppola, J. M., Ross, B. D., and Rehemtulla, A. (2008) Noninvasive imaging of apoptosis and its application in cancer therapeutics. *Clin. Cancer Res.* **14,** 2492–2501
11. Terme, M., Ullrich, E., Delahaye, N. F., Chaput, N., and Zitvogel, L. (2008) Natural killer cell-directed therapies: moving from unexpected results to successful strategies. *Nat. Immunol.* **9,** 486–494
12. Yan, Y., Steinherz, P., Klingemann, H. G., Dennig, D., Childs, B. H., McGuirk, J., and O'Reilly, R. J. (1998) Antileukemia activity of a natural killer cell line against human leukemias. *Clin. Cancer Res.* **4,** 2859–2868

13. Tam, Y. K., Martinson, J. A., Doligosa, K., and Klingemann, H. G. (2003) Ex vivo expansion of the highly cytotoxic human natural killer-92 cell-line under current good manufacturing practice conditions for clinical adoptive cellular immunotherapy. *Cytotherapy* **5,** 259–272
14. Ashkenazi, A., Pai, R. C., Fong, S., Leung, S., Lawrence, D. A., Marsters, S. A., Blackie, C., Chang, L., McMurtrey, A. E., Hebert, A., DeForge, L., Koumenis, I. L., Lewis, D., Harris, L., Bussiere, J., Koeppen, H., Shahrokh, Z., and Schwall, R. H. (1999) Safety and antitumor activity of recombinant soluble Apo2 ligand. *J. Clin. Invest.* **104,** 155–162
15. Lin, T., Huang, X., Gu, J., Zhang, L., Roth, J. A., Xiong, M., Curley, S. A., Yu, Y., Hunt, K. K., and Fang, B. (2002) Long-term tumor-free survival from treatment with the GFP-TRAIL fusion gene expressed from the hTERT promoter in breast cancer cells. *Oncogene* **21,** 8020–8028
16. Jacob, D., Davis, J., Zhu, H., Zhang, L., Teraishi, F., Wu, S., Marini, F. C., 3rd, and Fang, B. (2004) Suppressing orthotopic pancreatic tumor growth with a fiber-modified adenovector expressing the TRAIL gene from the human telomerase reverse transcriptase promoter. *Clin. Cancer Res.* **10,** 3535–3541
17. Muller, T., Uherek, C., Maki, G., Chow, K. U., Schimpf, A., Klingemann, H. G., Tonn, T., and Wels, W. S. (2008) Expression of a CD20-specific chimeric antigen receptor enhances cytotoxic activity of NK cells and overcomes NK-resistance of lymphoma and leukemia cells. *Cancer Immunol. Immunother.* **57,** 411–423
18. Nagashima, S., Mailliard, R., Kashii, Y., Reichert, T. E., Herberman, R. B., Robbins, P., and Whiteside, T. L. (1998) Stable transduction of the interleukin-2 gene into human natural killer cell lines and their phenotypic and functional characterization in vitro and in vivo. *Blood* **91,** 3850–3861
19. Reid, G. S., Bharya, S., Klingemann, H. G., and Schultz, K. R. (2002) Differential killing of pre-B acute lymphoblastic leukaemia cells by activated NK cells and the NK-92 ci cell line. *Clin. Exp. Immunol.* **129,** 265–271
20. Uherek, C., Tonn, T., Uherek, B., Becker, S., Schnierle, B., Klingemann, H. G., and Wels, W. (2002) Retargeting of natural killer-cell cytolytic activity to ErbB2-expressing cancer cells results in efficient and selective tumor cell destruction. *Blood* **100,** 1265–1273
21. Reefman, E., Kay, J. G., Wood, S. M., Offenhauser, C., Brown, D. L., Roy, S., Stanley, A. C., Low, P. C., Manderson, A. P., and Stow, J. L. (2010) Cytokine secretion is distinct from secretion of cytotoxic granules in NK cells. *J. Immunol.* **184,** 4852–4862
22. Dai, C., and Krantz, S. B. (1999) Interferon gamma induces upregulation and activation of caspases 1, 3, and 8 to produce apoptosis in human erythroid progenitor cells. *Blood* **93,** 3309–3316
23. Nowosielska, E. M., Cheda, A., Wrembel-Wargocka, J., and Janiak, M. K. (2011) Anti-neoplastic and immunostimulatory effects of low-dose X-ray fractions in mice. *Int. J. Radiat. Biol.* **87,** 202–212
24. Ishikawa, E., Tsuboi, K., Saijo, K., Takano, S., and Ohno, T. (2004) X-irradiation to human malignant glioma cells enhances the cytotoxicity of autologous killer lymphocytes under specific conditions. *Int. J. Radiat. Oncol. Biol. Phys.* **59,** 1505–1512
25. Hori, T., Kondo, T., Kanamori, M., Tabuchi, Y., Ogawa, R., Zhao, Q. L., Ahmed, K., Yasuda, T., Seki, S., Suzuki, K., and Kimura, T. (2010) Ionizing radiation enhances tumor necrosis factor-related apoptosis-inducing ligand (TRAIL)-induced apoptosis through up-regulations of death receptor 4 (DR4) and death receptor 5 (DR5) in human osteosarcoma cells. *J. Orthop. Res.* **28,** 739–745
26. Jeon, Y. H., Choi, Y., Kim, C. W., Kim, Y. H., Youn, H., Lee, J., and Chung, J. K. (2010) Human sodium/iodide symporter-mediated radioiodine gene therapy enhances the killing activities of CTLs in a mouse tumor model. *Mol. Cancer Ther.* **9,** 126–133
27. Ramakrishnan, R., Assudani, D., Nagaraj, S., Hunter, T., Cho, H. I., Antonia, S., Altiok, S., Celis, E., and Gabrilovich, D. I. (2010) Chemotherapy enhances tumor cell susceptibility to CTL-mediated killing during cancer immunotherapy in mice. *J. Clin. Invest.* **120,** 1111–1124
28. Melder, R. J., Brownell, A. L., Shoup, T. M., Brownell, G. L., and Jain, R. K. (1993) Imaging of activated natural killer cells in mice by positron emission tomography: preferential uptake in tumors. *Cancer Res.* **53,** 5867–5871

Received for publication October 27, 2013.
Accepted for publication March 17, 2014.